Research Article

Highly efficient cathode for the microbial fuel cell using $LaXO_3$ (X = [Co, Mn, $Co_{0.5}Mn_{0.5}$]) perovskite nanoparticles as electrocatalysts

Fatemeh Nourbakhsh[1,2,5] · Mohsen Mohsennia[1,3] · Mohammad Pazouki[4]

Received: 25 June 2019 / Accepted: 15 January 2020 / Published online: 12 February 2020

Abstract

Non-precious metal catalysts are needed for the commercialization of microbial fuel cells (MFCs). Therefore, in this work, we synthesized the cost-effective $LaCoO_3$, $LaMnO_3$, and $LaCo_{0.5}Mn_{0.5}O_3$ perovskite-type oxide nanoparticles, as cathode catalysts, and replaced them by the platinum (Pt) cathode. The high electro-catalytic efficiency of the perovskite catalysts was determined by the linear sweep voltammetry, Tafel plot and electrochemical impedance spectroscopy analyses. The maximum power density obtained by the $LaMnO_3$ was determined to be higher than 13.91 mW m^{-2}, which is more than twice as high as that obtained by the carbon cloth cathode under identical conditions. Also, the maximum power density of MFC with the modified electrodes was more than twice as high as that of the pristine cathode and 5.2% lower than Pt. Therefore, the prepared perovskite-type oxide nanoparticles can be used as efficient catalysts for the oxygen reduction reaction (ORR) in a two-chamber MFCs.

Graphic abstract

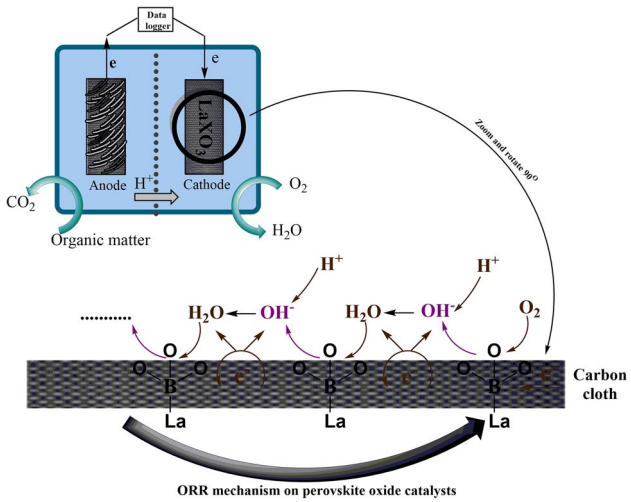

Keywords Cathodic catalyst · Electrocatalysis · La-based perovskite oxide · Microbial fuel cell

✉ Fatemeh Nourbakhsh, fnourbakhsh@nri.ac.ir | [1]Department of Chemistry, University of Kashan, Kashan, Iran. [2]Young Researchers and Elite Club, Karaj Branch, Islamic Azad University, Karaj, Iran. [3]Institute of Nanoscience and Nanotechnology, University of Kashan, Kashan, Iran. [4]Department of Energy, Institute of Materials and Energy (MERC), Meshkindasht, Karaj, Iran. [5]Non-Metallic Materials Research Group, Niroo Research Institute, End of Dadman Street, Kashan, Tehran Province 1468613113, Iran.

SN Applied Sciences (2020) 2:391 | https://doi.org/10.1007/s42452-020-2048-1

1 Introduction

Microbial fuel cell (MFC) technology has the incomparable potential for the electricity production from a broad range of wastewaters. The electrode limitations are among the most important drawbacks, which limits the practical application of MFC technology [1, 2]. The cathode as a destination for electrons and protons is the major limiting factor for the current generation. Also, the cathode price is crucial in total cost of MFCs. In fact, the main limitation of the cathode is related to the slow reaction kinetics of the oxygen reduction. The use of economical cathode catalysts to improve the electrocatalytic properties has frequently been studied in the literature [3].

Among abiotic cathodes, three main groups can be classified into three main categories: carbonaceous materials, platinum group metal (PGM) and Platinum group metal-free (PGM-free) catalysts. PGM-free materials based on the combining of transition metals such as Fe, Co, Mn, V, and Ni have been used as cathode catalyst [4–7]. Recent research shows that transition metals and their oxides due to abundant availability on the earth, high durability, low cost and high activity exhibited remarkable catalytic activity for ORR in MFC [7–9]. Since transition metals are known to have a considerable electrochemical activity, these results imply that the bi- or tri-metallic oxides show excellent catalytic activity towards ORR [10–12].

It has been proposed that the perovskites as the bimetallic oxides, belonging to ABO_3 category can be used as low-cost catalysts for the oxygen reduction reaction (ORR) due to their very fast-charge and -discharge ability [13, 14]. The best performance on the ORR activity is obtained by the lanthanum (La) as the A-site cation. The different valence states of B-site cation, and therefore, the multiplicity redox couples of catalysts enhance the activity of the perovskite-type catalysts used in the ORR [15]. Based on some new studies, it has been revealed that perovskite-carbon nanocomposites are good candidates for the ORR in MFCs [16, 17].

This article is focused on the synthesis and characterization of bimetallic Co-Mn oxides with La-based perovskite oxides, $LaXO_3$ (X = Co, Mn, and $Co_{0.5}Mn_{0.5}$), structure to achieve cobalt and manganese redox couples as ORR catalysts used in the cathode of MFC. The electro-catalytic properties of La-based perovskite oxides were investigated in 50 mmol l^{-1} phosphate buffer solution as an electrolyte (pH = 6.8) at 28 ± 2 °C. The electrochemical tests were done through linear sweep voltammetry (LSV) and Tafel plots. Furthermore, the internal resistance of the MFC in the presence of the $LaMnO_3$ coated cathode was determined by the electrochemical impedance spectroscopy (EIS).

2 Experimental

2.1 Catalysts synthesis and characterization

La, Mn and Co nitrates were used in the stoichiometric amount to synthesize the $LaXO_3$ catalysts using the sol–gel method. At first, 3.5 mmol of $La(NO_3)_3{\cdot}6H_2O$ and 3.5 mmol of $Mn(NO_3)_2{\cdot}4H_2O$ for $LaMnO_3$ (LM) [18]; 3.5 mmol of $La(NO_3)_3{\cdot}6H_2O$ and 3.5 mmol of Co $(NO_3)_2{\cdot}6H_2O$ for $LaCoO_3$ (LC) [19]; and 3.5 mmol of $La(NO_3)_3{\cdot}6H_2O$, 1.75 mmol of $Mn(NO_3)_2{\cdot}4H_2O$ and 1.75 mmol of $Co(NO_3)_2{\cdot}6H_2O$ for $LaMn_{0.5}Co_{0.5}O_3$ (LMC) were added to heated propionic acid solution. Then, the obtained uniform solutions were refluxed to obtain a gel. The solutions were dried at 80 °C for 48 h and the resultant materials were calcined at 750 °C for 4 h under air atmosphere [20]. The Philips X-ray diffractometer PW 3710 equipped with Cu $K\alpha_1$ radiation ($\lambda = 0.154$ nm) was used for the evaluation of the crystalline structure of the synthesized catalysts (step scan range = $10 \le 2\theta \le 90°$, scan rate = 0.02° min^{-1} at 28 ± 2 °C). The X'Pert high score plus 2.2b software was used for the identification of various phases of XRD patterns. The morphology of the catalysts was studied by Cambridge 1990, S 360 scanning electron microscopy (SEM).

2.2 Electrode fabrication

The carbon cloth (the tensile strength of 3530 MPa, 205 ± 15 microns thick) was used as the MFC electrodes with the projected surface area of 32 cm^2 (plain, T-300, Toray). The cathode catalysts of 10% catalyst/Carbon were coated in carbon cloth (0.5 mg of Pt or La-based perovskite catalysts per 1 cm^2 of the cathode surface area) (Pt particle size 0.5–1.2 µm, Sigma-Aldrich). The catalyst paste-like mixture was prepared by 0.83 µl of deionised water (DI water) and 6.67 µl of binder solution (polytetrafluoroethylene 60 wt%, Sigma-Aldrich) for every 1 mg of catalyst/Carbon and sonicated and brushed on the carbon cloth (CC) at room temperature for 24 h.

2.3 MFC tests

The two chamber MFC was constructed using two cubic plexiglass chambers (10 cm × 6 cm × 6 cm) with the approximate working volume of 450 ml. The Nafion-117 (Sigma Aldrich) was used as a membrane. Prior to use,

the membrane and electrodes were regenerated and then the cathode was coated by the catalysts. The oxygen was injected to the cathode compartment as an electron acceptor (rate = 2.5 l h^{-1}). The carbon cloth was used as the MFC anode without the catalyst layer. The anolyte was 0.5 g l^{-1} sodium acetate and 2.5% MH (Mueller–Hinton) medium at pH = 8. The MH medium contains 0.5 g glucose l^{-1}, 10 g yeast extract l^{-1}, 2.5 g peptone l^{-1}, 20.25 g NaCl l^{-1}, 1.75 g $MgCl_2$ l^{-1}, 2.40 g $MgSO_4$ l^{-1}, 0.5 g KCl l^{-1}, 90 mg $CuCl_2$ l^{-1}, and 6.5 mg NaBr l^{-1}. The anolyte was inoculated with the pure culture of *Shewanella* Sp. IBRC-M 4029.

2.4 Electrochemical measurements

Electro-catalytic performances of the prepared catalysts were evaluated using LSV and Tafel plots after 7 days. Open circuit voltages were measured using a 289 Fluke true RMS multimeter every 20 min and the polarization curves before the electrochemical tests were also obtained. The performance of an MFC was evaluated through the power output as described elsewhere [21]. LSV and EIS experiments were performed by using an Autolab, PGSTAT30 potentiostat/galvanostat. The electrochemical analysis of the cathode was characterized using a three-electrode mode [22].

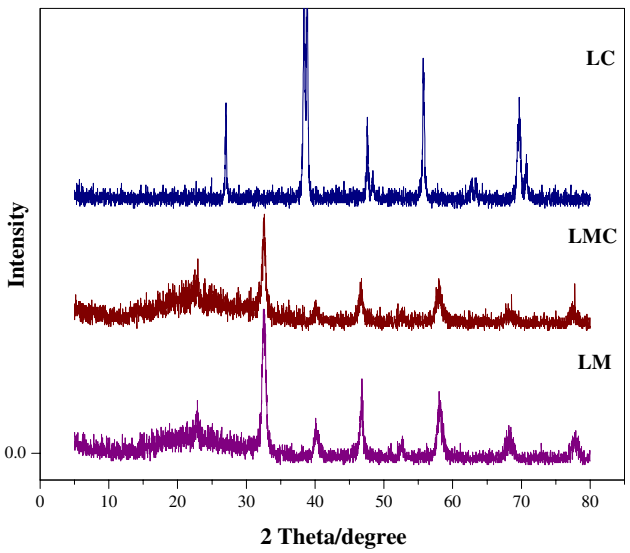

Fig. 1 XRD patterns of LM, LMC and LC

3 Results and discussion

3.1 Characterization of the catalyst

The crystalline phases of the prepared perovskites were studied by X-ray diffraction spectroscopy (XRD) analyses (Fig. 1). The major peaks of the LC at 2θ = 27.04, 38.27, 38.86, 47.62, 48.42, 55.73, 62.00, 63.40, 69.17, 69.75, 70.79, 82.26 and 83.46° indicate a rhombohedral arrangement with the space group $R\bar{3}C$ (powder diffraction file No. 01-084-0848). Another set of peaks at 2θ = 22.82, 32.47, 40.09, 46.72, 52.65, 58.15, 68.29 and 77.65° belong to cubic LM with the space group $Pm\bar{3}m$ (powder diffraction file No. 01-075-0440) [23]. The XRD spectrum of the LMC shows an orthorhombic crystal structure with the space group Pbnm. According to the obtained results listed in Table 1, the perovskite-type structure was preserved after the partial substitution of Mn into the pristine structure of LC. In fact, the perovskite oxides can easily accept dopant cations and have high tolerance to changes upon the addition of either A or B cations.

A Field emission scanning electron microscope (FESEM) images are shown in Fig. 2. Accordingly, the porous particles are around 30–72 nm. The obtained LM and LMC particles became more agglomerated, which indicate the smaller particle size in comparison with LC. These findings are also in good agreement with the XRD results. The XRD peaks of LM and LMC are broader than the corresponding XRD peaks of LC, which can be indicative of the smaller size of the LM and LMC particles. The distributions of the local composition of LMC has examined by the Energy-dispersive X-ray spectroscopy (EDS) technique. The EDS results (as shown in Fig. 2g) indicate the incorporation of the elements La, Mn, Co and oxygen into the LMC composition. According to the EDS results, the LMC composition is stoichiometric and impurity elements were not observed.

3.2 Electrocatalytic activity of the synthesized LM catalyst

The electrochemical activities of the electrodes (carbon cloth, carbon cloth coated with LM catalyst as the most

Table 1 Phase identification and symmetry from X-ray diffraction patterns

Perovskite	PDF no.	Crystal structure	Space group (no.)	a (Å)	b (Å)	c (Å)
LC	01-084-0848	Rhombohedral	$R\bar{3}c$ (167)	5.3778	5.3778	5.3778
LM	01-075-0440	Cubic	$Pm\bar{3}m$ (221)	3.88	3.88	3.88
LMC	01-072-1186	Orthorhombic	Pbnm (62)	5.5250	5.5300	7.8190

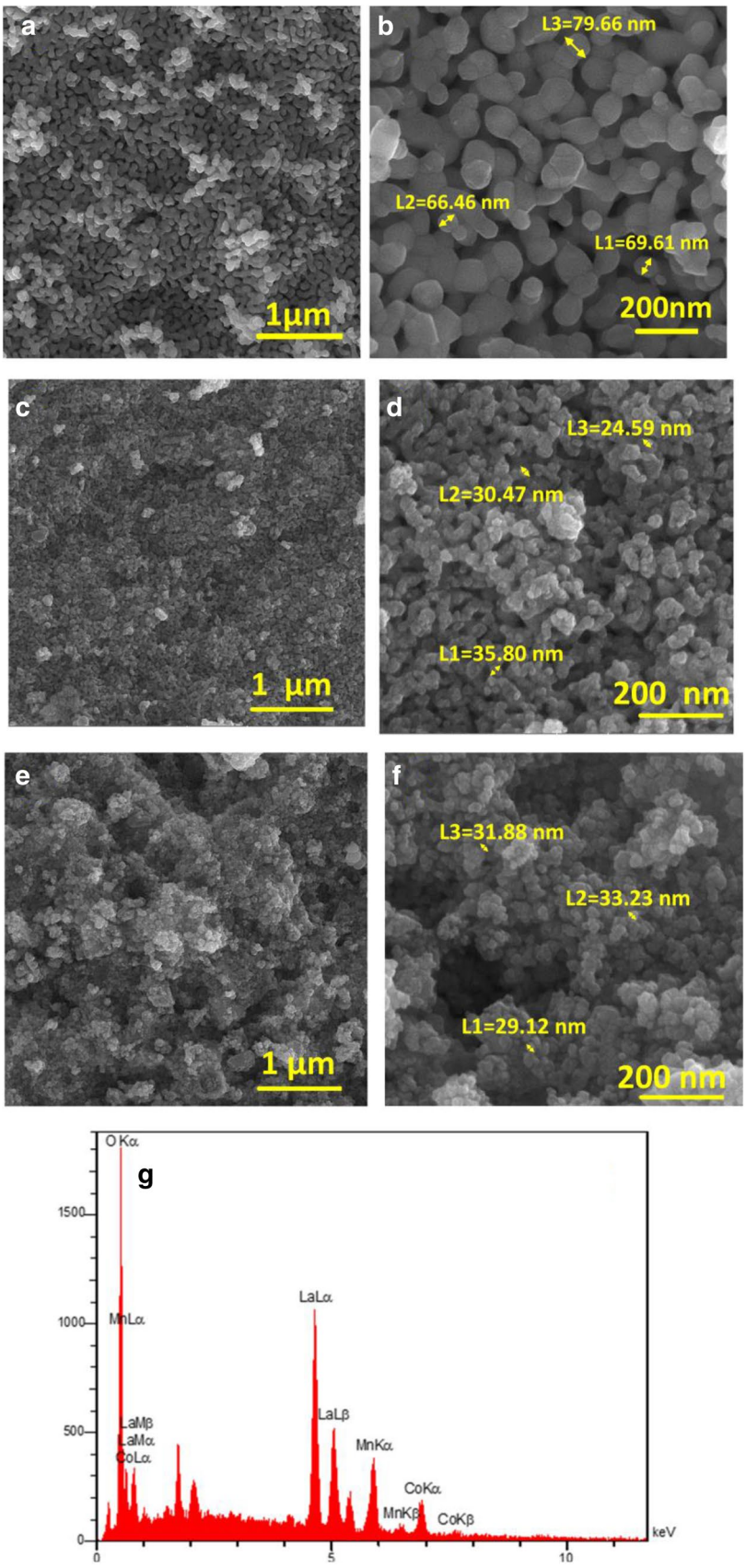

Fig. 2 FESEM images of **a**, **b** LC and approximation of particle size of LC, **c**, **d** LM, **e**, **f** LMC and **g** EDS results of LMC

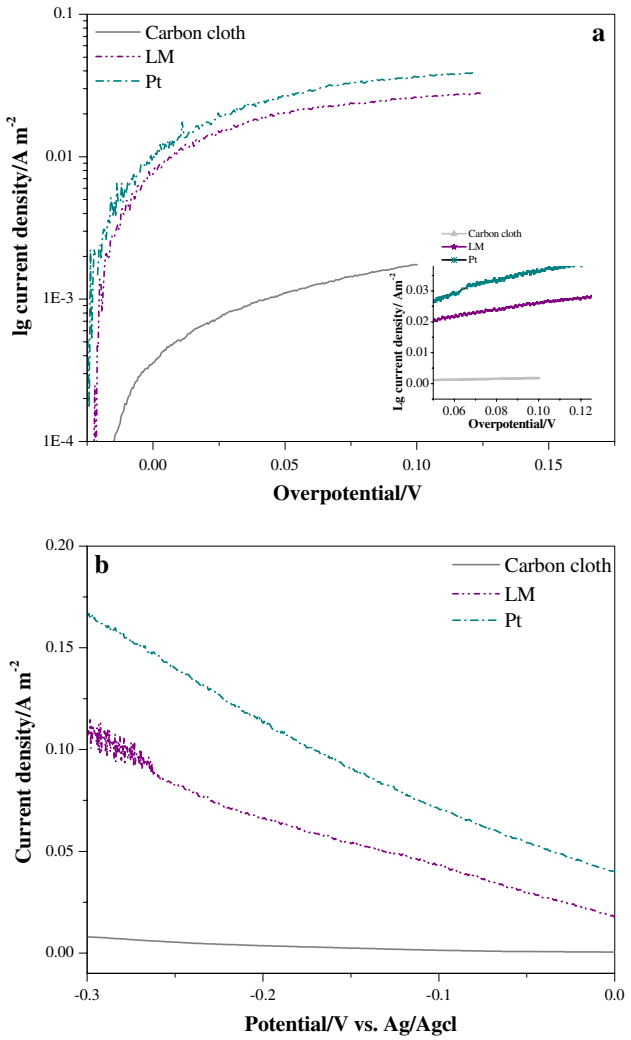

Fig. 3 **a** Tafel plots of O_2 (from air) reduction obtained in phosphate buffer at scan rate 1 mV S^{-1} and the inset is the linear fit for the overpotential from 50 to 125 mV. **b** Line sweep voltammograms of O_2 (from air) reduction obtained in phosphate buffer at scan rate 1 mV S^{-1}

efficient synthesized catalyst and Pt) in a phosphate buffer (pH = 6.8) were investigated by LSV and Tafel plots (Fig. 3). According to LSV results, the significant electrochemical reaction was not observed for the pristine cathode in the selected potential. The redox characteristic of pristine carbon cloth was improved by LM as shown in Fig. 3a, b. The LM/CC showed good catalytic activity to the ORR compared with the Pt/CC and CC cathodes.

Three different reduction peaks were observed in the LSV results of the CC and LM/CC cathodes. However, the current peak resulted by the LM/CC was higher than the other peaks, which is because of the facilitating effect on the ORR via the proposed 4-electron pathway mechanism of La-based perovskite oxide catalysts in the literatures [25]. Based on literature, perovskite type oxides are known for promising ORR catalytic activity because of their flywheel effect [26].

4electron pathway mechanism of Pt catalyst lead to strong kinetic activity of ORR and 2electron ORR of CC result into mild kinetic activity. According to Yu and Wang studies [22], the La-based perovskite like LM may catalyze ORR by hybrid pathway near to 4electron. This could be confirm the LSV results.

The kinetics of charge transfer over-potentials was described by Tafel analysis based on Bulter–Volmer equation. At an electrode at equilibrium, the exchange current density (j_0) is a crucial parameter in the rate of electro-reduction or electro-oxidation of chemical species (Eq. 1) [27]. For cathodic reaction:

$$\log|j| = \log|j_0| - \alpha_c(nF/2.303RT)\eta \quad (1)$$

where j is the total current density, α_c is the cathodic Tafel slope and η is the over-potential. j_0 can be determined over the linear region of the Tafel plots (over-potential from 50 to 125 mV) as shown in Fig. 3a. The exchange current densities of 1.001 and 1.039 A m^{-2} were calculated for CC and LM/CC, respectively. At equilibrium, j_0 represents the rate of exchange between the product and reactant. A higher value of j_0 means a faster reaction rate. Therefore, the higher exchange current density of the fabricated LM/CC indicates a faster reaction rate at the electrode in comparison with the CC electrode. Thereby the LM can be considered as the suitable cathode catalyst in MFCs [22]. Gasteiger et al. [24] have reported the highest ORR activity of perovskite oxide catalysts correlate to e_g occupation of transition metals in B site. Moderate e_g filling in LM (Mn, $e_g = 1$) can lead to high activity of ORR. The high current reduction peak and high value of j_0 of LM/CC can be resulted from rate-limiting step in proposed ORR mechanism [28].

Owing to the superiority of the prepared LM catalyst, the EIS analysis was used to investigate the effect of internal resistance (R_{in}) on the MFC performance in the presence of LM/CC cathode in comparison with the pristine cathode. The Nyquist plots are shown in Fig. 4.

The Randles equivalent circuit (Fig. 5) consists of R_S (an electrolyte solution resistance) in series with the parallel circuit of a C_{dl} (double-layer capacitance) and an impedance of a faradaic charge-transfer reaction (including an active charge transfer resistance R_{ct} and the Warburg element) [29]. The Nyquist plots of both LM coated and bare cathodes represent a charge transfer resistance (R_{ct}) at the electrode/electrolyte interface (diameter of the semicircle) [30]. As can be observed in Fig. 6, the R_{ct} of the LM/CC was remarkably smaller than that of the CC, which shows the faster electron transfer rate of the modified coated cathode in comparison with the pristine

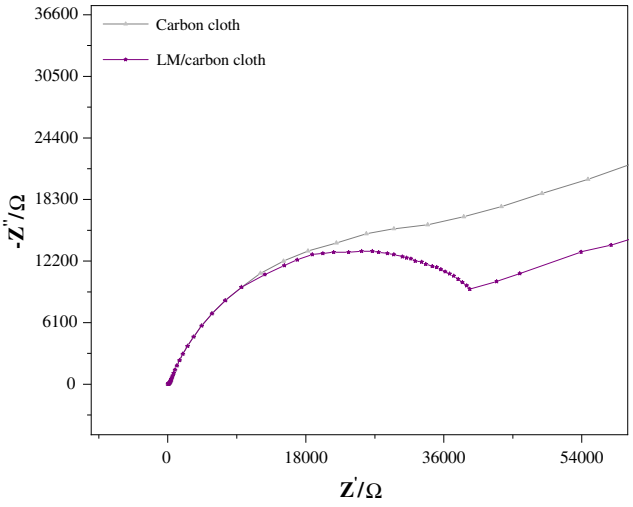

Fig. 4 Comparison of Nyquist plots of the LM perovskite and bare carbon cloth cathodes in an anaerobic suspension of *Shewanella* containing MH medium with acetate

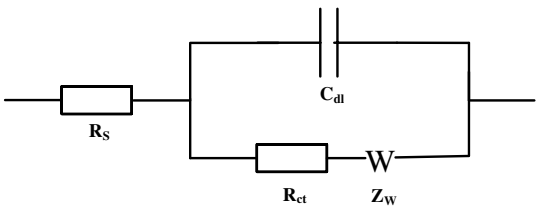

Fig. 5 Schematic equivalent circuit model for EIS data fitting

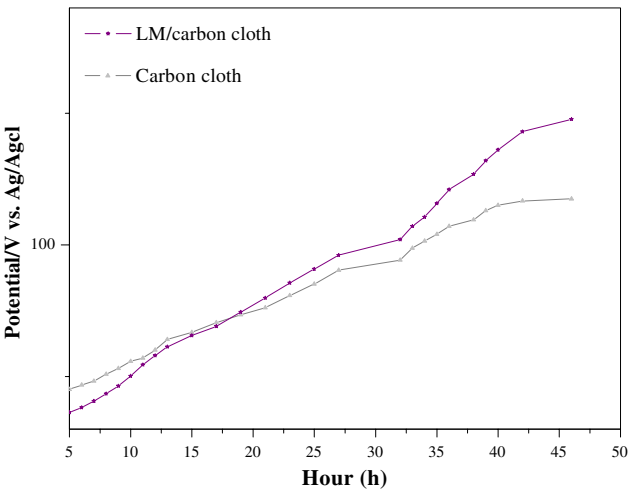

Fig. 6 Potential-time curves of MFC utilizing LM perovskite electrode and bare carbon cloth as a cathode versus Ag/AgCl reference electrode

electrode [30]. These results are in agreement with the Tafel results.

Figure 6 shows the cathode electrode potential versus an Ag/AgCl reference electrode (RE) plotted against discharge time. The higher potential in the plot represents the catalytic performance of the LM perovskite catalyst. According to Fig. 6, the more potential 147.7 V versus RE of the LM/CC cathode compared to 117.5 V versus RE of the bare cathode demonstrates an acceptable electro-catalytic activity of the modified LM perovskite cathode, which is in accordance with the LSV results. According to the electro-chemical results, it seems that the low-cost La-based perovskite-type nanocatalysts, especially LM ones, are suitable to be used as cathode catalysts in MFCs [22].

3.3 Performance in MFCs

The maximum power density of the pristine electrode was improved by the perovskite oxide catalysts. The power density curve of the different catalysts as a function of current density is shown in Fig. 7a. The high power density observed for the perovskite oxide catalysts is indicative of their excellent catalytic activities. As expected, the maximum power densities were achieved by MFC with the catalysts in the order of LM (13.91 mW m^{-2}, 120% compare to CC), LMC (8.78 mW m^{-2}, 39% compare to CC), LC (6.99 mW m^{-2}, 11% compare to CC) and the pristine cathode (CC) (6.30 mW m^{-2}). The maximum power density of the LM perovskite oxide-based MFC was about two times higher than that of the carbon cloth-based MFC. Table 2 shows the comparative results obtained from MFCs. The voltages measured during the current generation are plotted in Fig. 7b.

The order of the internal resistance for the fabricated MFCs with different cathode electrodes is CC > LC > LMC > LM. The decrease of the internal resistance may be due to the fact that the La-based perovskites, especially LM, have a great effect on the decrease of the activation energy of ORR at neutral medium, which improves the perovskite catalyst reaction [22]. Moreover, the electro-catalytic activity of the perovskites is definitely correlated with the charge of the transition metal cation and its valence state during the ORR [24]. The performance of the studied La-based perovskite catalysts are compared in Fig. 8. Accordingly, the modification of the cathode leads to the increase of the maximum power density of the MFC by 10% and 120% for the LC and LM, respectively. Also, the current density output increases by 14% and 134% for the LC and LM, respectively, while the internal resistance decreases by 29% and 54%.

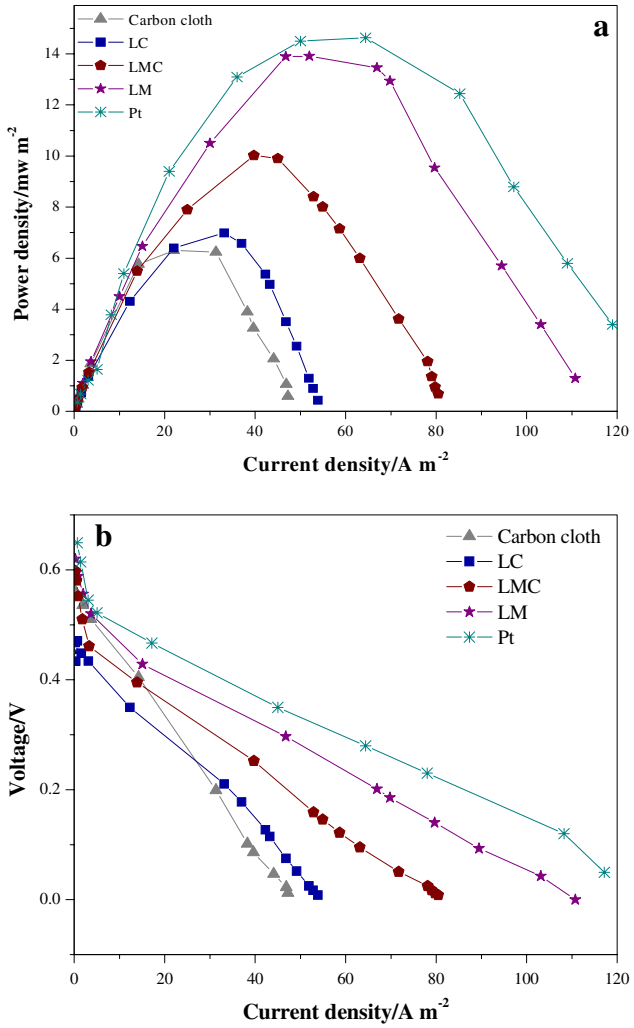

Fig. 7 MFC **a** polarization curves and **b** power density curves of different electrodes

Table 2 Internal resistances, maximum power densities, maximum current densities and open circuit voltages (OCVs) at steady state (SS) condition of the MFCs

Perovskite	CC[a]	LC/CC	LMC/CC	LM/CC	Pt/CC
MPD[b] (mW m^{-2})	6.30	6.99	8.78	13.91	14.63
MCD[c] (mA m^{-2})	47.25	53.85	80.46	110.79	117.18
MV[d] (mV)	592.15	613.84	634.30	656.24	689.31
IR[e] (Ω m^{-2})	11.69	8.23	6.78	5.39	4.52

[a]Carbon cloth cathode

[b]Maximum power density

[c]Maximum current density

[d]Maximum voltage

[e]Internal resistance

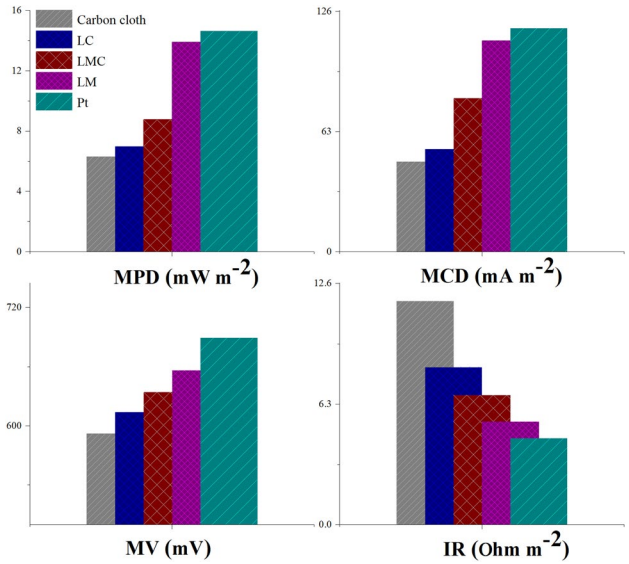

Fig. 8 An column/bar diagram of the obtained results of the MFC with La-based perovskite catalyst in comparison with bare and Pt-coated carbon cloth cathode

4 Conclusion

The La-based perovskite-type oxide nanoparticles were synthesized and examined for their catalytic behavior in a dual-chambered MFC as cathode catalysts. The structure and morphology of the synthesized La-based perovskite catalysts were studied by XRD and FESEM. Also, their electrochemical properties were investigated by LSV, EIS and Tafel plots in the phosphate buffer solution at pH = 6.8 and 28 ± 2 °C. According to the obtained results, the electrocatalytic activity of the carbon cloth coated La-based perovskite oxides towards the ORR increased and a higher power production was observed. Furthermore, it was shown that the LM/CC as an efficient cathode catalyst for the ORR in a dual-chamber MFCs, exhibits a maximum power density of 13.91 mW m^{-2}, 120% higher than CC.

It has been estimated that the cost of $LaXO_3$ (X = [Co, Mn, $Co_{0.5}Mn_{0.5}$]) is in average 0.05 $\$g^{-1}$ in compare to ~ 18 $\$g^{-1}$ Pt. Thereby MPDs of $LaXO_3$ compared to Pt is speculated to be 4.1 mWm^{-2} $\$^{-1}$ to 0.16 mWm^{-2} $\$^{-1}$. Therefore, it can be concluded that due to the low-cost, easier preparation method and excellent electrocatalytic activity, La-based perovskite catalysts, especially the prepared LM nanoparticles, can be considered as a cathode catalyst in MFCs.

The future Studies will include the investigation of ORR activity of La-based perovskite catalyst with different transmition metals in B site.

Acknowledgements We would like to thank the Iranian National Science Foundation (INSF) with the research proposal number 89001989.

Compliance with ethical standards

Conflict of interest The authors declare that they have no conflict of interest.

References

1. Rabaey K, Angenent L, Schroder U, Keller J (2009) Bioelectrochemical systems: from extracellular electron transfer to biotechnological application. In: Biotechnology application. IWA Publishing, London, pp 137–152. https://doi.org/10.1007/s00449-2016876
2. Nourbakhsh F, Mohsennia M, Pazouki M (2017) Nickel oxide/carbon nanotube/polyaniline nanocomposite as bifunctional anode catalyst for high-performance Shewanella-based dual-chamber microbial fuel cell. Bioprocess Biosyst Eng 40:1669–1677. https://doi.org/10.1007/s00449-017-1822-y
3. Zhang X, Li K, Yan P, Liu Z, Pu L (2015) N-type Cu_2O doped activated carbon as catalyst for improving power generation of air cathode microbial fuel cells. Bioresour Technol 187:299–304. https://doi.org/10.1016/j.biortech.2015.03.131
4. Cao C, Wei L, Wang G, Shen J (2017) Superiority of boron, nitrogen and iron ternary doped carbonized graphene oxide-based catalysts for oxygen reduction in microbial fuel cells. Nanoscale 9:3537–3546. https://doi.org/10.1039/C7NR00869D
5. Luo S, He Z (2016) Ni-coated carbon fiber as an alternative cathode electrode material to improve cost efficiency of microbial fuel cells. Electrochim Acta 222:338–346. https://doi.org/10.1016/j.electacta.2016.10.178
6. Xu X, Dai Y, Yu J, Hao L, Duan Y, Sun Y, Zhang Y, Lin Y, Zou J (2017) Metallic state FeS anchored (Fe)/Fe_3O_4/N-doped graphitic carbon with porous spongelike structure as durable catalysts for enhancing bioelectricity generation. ACS Appl Mater Interfaces 9:10777–10787. https://doi.org/10.1021/acsami.7b01531
7. Ayyaru S, Mahalingam S, Ahn YH (2019) A non-noble V_2O_5 nanorods as an alternative cathode catalyst for microbial fuel cell applications. Int J Hydrog Energy 44(10):4974–4984. https://doi.org/10.1016/j.ijhydene.2019.01.021
8. Goenaga RA, Cantillo NM, Foister S, Zawodzinski TA (2018) A family of platinum group metal-free catalysts for oxygen reduction in alkaline media. J Power Sources 395:148–157. https://doi.org/10.1016/j.jpowsour.2018.05.025
9. Gokhale R, Tsui L-K, Roach K, Chen Y, Hossen MM, Artyushkova K, Garzon F, Atanassov P (2018) Hydrothermal synthesis of platinum-group-metal-free catalysts: structural elucidation and oxygen reduction catalysis. ChemElectroChem 5:1848–1853. https://doi.org/10.1002/celc.201700949
10. Guoa X, Jiab J, Donga H, Wanga Q, Xua T, Fua B, Ranb R, Lianga P, Huanga X, Zhanga X (2019) Hydrothermal synthesis of FeeMn bimetallic nanocatalysts as highefficiency cathode catalysts for microbial fuel cells. J Power Sources 414:444–452. https://doi.org/10.1155/2014/791672
11. Indrasis D, Noori T, Gourav DB (2018) Synthesis of bimetallic iron ferrite $Co_{0.5}Zn_{0.5}Fe_2O_4$ as a superior catalyst for oxygen reduction reaction to replace noble metal catalysts in microbial fuel cell. Int J Hydrog Energy 43(41):19196–19205
12. Zhang S, Su W, Wang X, Li K, Li Y (2019) Bimetallic metal-organic frameworks derived cobalt nanoparticles embedded in nitrogen-doped carbon nanotube nanopolyhedra as advanced electrocatalyst for high-performance of activated carbon air-cathode microbial fuel cell. Biosens Bioelectron 15(17):181–187. https://doi.org/10.1016/j.bios.2018.12.028
13. Kéranguéven G, Royer S, Savinova E (2015) Synthesis of efficient Vulcan–$LaMnO_3$ perovskite nanocomposite for the oxygen reduction reaction. Electrochem Comm 50:28–31. https://doi.org/10.1016/j.elecom.2014.10.019
14. Farahani FS, Mecheri B, Majidi MR, Placidi E, Epifanio A (2019) Carbon-supported Fe/Mn-based perovskite-type oxides boost oxygen reduction in bioelectrochemical systems. Carbon 145:716–724. https://doi.org/10.1016/j.carbon.2019.01.083
15. Jorissen L (2006) Bifunctional oxygen/air electrodes. J Power Sources 155:23–32
16. Bai LJ, Wang XY, He HB, Guo QJ (2014) Preparation and characteristics of LAXSR1-XCOO3 as cathode catalysts for microbial fuel cell. In: Particle science and engineering: proceedings of UK-China International Particle Technology Forum IV. The Royal Society of Chemistry, pp 15–21. https://doi.org/10.1039/9781782627432-00015
17. Nourbakhsh F, Pazouki M, Mohsennia M (2017) Impact of modified electrodes on boosting power density of microbial fuel cell for effective domestic wastewater treatment: a case study of Tehran. J Fuel Chem Technol 45(7):871–879. https://doi.org/10.1016/S1872-5813(17)30041-5
18. Dumas C, Basseguy R, Bergel A (2008) Electrochemical activity of Geobacter, sulfurreducens biofilms on stainless steel anodes. Electrochim Acta 53:5241. https://doi.org/10.1016/S0013-4686
19. Kumar GG, Sarathi VG, Nahm KS (2010) Recent advances and challenges in the anode architecture and their modifications for the applications of microbial fuel cells. Biosens Bioelectron 43:461–475. https://doi.org/10.1016/j.bios.2012.12.048
20. Moradi GR, Rahmanzadeh M, Sharifnia S (2010) Kinetic investigation of CO_2 reforming of CH_4 over La–Ni based perovskite. Chem Eng J 162:787–791. https://doi.org/10.1016/j.cej.2010.06.006
21. Logan BE, Aelterman P, Hamelers B, Rozendal R, Schröer U, Keller J, Freguia S, Verstraete W, Rabaey K (2006) Microbial fuel cells: methodology and technology. Environ Sci Technol 40:5181–5192. https://doi.org/10.1021/es0605016
22. Dong H, Yu H, Wang X, Zhou Q, Sun J (2012) Carbon-supported perovskite oxides as oxygen reduction reaction catalyst in single chambered microbial fuel cells. J Chem Technol Biotechnol 88:774–778. https://doi.org/10.1002/jctb.3893
23. Magalhãesa F, Camilo Mourab FC, Ardissonc JD, Lagoa RM (2008) $LaMn_{1-x}Fe_xO_3$ and $LaMn_{0.1-x}Fe_{0.90}Mo_xO_3$ perovskites: synthesis, characterization and catalytic activity in H_2O_2 reactions. Mater Res 11(3):307–312
24. Suntivich J, Gasteiger HA, Yabuuchi N, Nakanishi H, Goodenough JB, Shao-Horn Y (2011) Design principles for oxygen-reduction activity on perovskite oxide catalysts for fuel cells and metal–air batteries. Nat Chem 3:546–550. https://doi.org/10.1038/nchem.1069
25. Kinoshita K (1990) Particle size effects for oxygen reduction on highly dispersed platinum in acid electrolytes. J Electrochem Soc 137(3):845–848. https://doi.org/10.1149/1.2086566
26. Tulloch J, Donne SW (2009) Activity of perovskite $La_{(1-X)}Sr_{(X)}MnO_3$ catalysts toward oxygen reduction in alkaline electrolytes. J Power Sources 188:359–366

27. Manohar AK, Bretschger O, Nealson KH, Mansfeld F (2008) The polarization behavior of the anode in a microbial fuel cell. Electrochim Acta 53:3508–3513. https://doi.org/10.1016/j.electacta.2007.12.002
28. Goodenough JB, Cushing BL (2003) Handbook of fuel cells, fundamentals technology and applications, vol 2. Wiley, New York, pp 520–533
29. Hsu CH, Mansfeld F (2001) Concerning the conversion of the constant phase element parameter Y_0 into a capacitance. Corrosion 57:747–748. https://doi.org/10.5006/1.3280607
30. Sekar N, Ramasamy RP (2013) Electrochemical impedance spectroscopy for microbial fuel cell characterization. J Microb Biochem Technol. https://doi.org/10.4172/1948-5948.s6-004